

## Absolute $\beta$ -to-ground band transition strengths in $^{154}\text{Sm}$

T. Möller,<sup>1,\*</sup> N. Pietralla,<sup>1</sup> G. Rainovski,<sup>1,2</sup> T. Ahn,<sup>1,3,†</sup> C. Bauer,<sup>1</sup> M. P. Carpenter,<sup>4</sup> L. Coquard,<sup>1</sup> R. V. F. Janssens,<sup>4</sup> J. Leske,<sup>1</sup> C. J. Lister,<sup>4</sup> E. A. McCutchan,<sup>4</sup> O. Möller,<sup>1</sup> D. Seweryniak,<sup>4</sup> and S. Zhu<sup>4</sup>

<sup>1</sup>*Institut für Kernphysik, Technische Universität Darmstadt, 64289 Darmstadt, Germany*

<sup>2</sup>*Faculty of Physics, St. Kliment Ohridski University of Sofia, 1164 Sofia, Bulgaria*

<sup>3</sup>*Wright Nuclear Structure Laboratory, Yale University, New Haven, Connecticut 06520, USA*

<sup>4</sup>*Physics Division, Argonne National Laboratory, Argonne, Illinois 60439, USA*

(Received 29 May 2012; revised manuscript received 2 August 2012; published 17 September 2012)

Low-lying collective states of  $^{154}\text{Sm}$  are studied via the  $^{12}\text{C}(^{154}\text{Sm}, ^{154}\text{Sm}^*)$  Coulomb excitation reaction at 85% of the Coulomb barrier (570 MeV) using the Gammasphere Ge-detector array. Absolute transition strengths are obtained from the Coulomb excitation cross sections deduced from the relative  $\gamma$ -ray yields. The results include transition strengths for  $E2$  decays of energy levels in the low-spin part of the first excited  $K^\pi = 0^+$  rotational band of  $^{154}\text{Sm}$ . The agreement of these results with the confined  $\beta$ -soft rotor model predictions establishes the assignment of this band as a  $\beta$  band.

DOI: [10.1103/PhysRevC.86.031305](https://doi.org/10.1103/PhysRevC.86.031305)

PACS number(s): 21.60.Ev, 23.20.-g, 25.70.De, 27.70.+q

Collective rotational excitations of heavy atomic nuclei represent an example of simple regular patterns emerging from the complex dynamical behavior of strongly interacting many-body Fermi systems. The collective behavior is expected also to result in simple selection rules for electromagnetic transitions. Despite their complexity, these states can qualitatively be understood, to a large extent, as resulting from surface vibrations or rotations of a drop of quantum liquid. The concept of nuclear shape is the cornerstone of geometrical collective models [1]. In the most important case of quadrupole shapes, the dynamics of the system is described by the Bohr Hamiltonian [1]. There are several analytically solvable cases of the geometrical Bohr Hamiltonian, e.g., the harmonic vibrator [ $R_{4/2} = E(4_1^+)/E(2_1^+) = 2.0$ ], the quadrupole-deformed axial rotor ( $R_{4/2} = 3.33$ ), the  $\gamma$ -unstable rotor ( $R_{4/2} = 2.5$ ) [2], and the  $\gamma$ -unstable,  $\beta$ -confined rotor [2–4]. Understanding the evolution of the nuclear shape and structure as a function of the nucleon number between these benchmarks of nuclear quadrupole collectivity is one of the most intriguing tasks of nuclear structure research. To an even larger extent this applies for the regions around the shape transitional points [3,5–7], which are characterized by large fluctuations of the quadrupole shape of the ground state.

The X(5) solution ( $R_{4/2} = 2.90$ ) describes a situation close to the shape phase transition from a spherical vibrator to a rigid rotor [5]. The X(5) solution, which was first applied to the deformed nucleus  $^{152}\text{Sm}$  [7], has revived a debate on the possible existence of  $\beta$ -vibrational bands. In the geometrical model, the  $\beta$  bandhead has been defined as an intrinsic vibrational excitation as a function of the quadrupole-deformation parameter  $\beta$  [8]. This one-phonon vibrational excitation features a wave function with one node as a function of  $\beta$ . Clearly, the first excited  $0^+$  state of the X(5) solution, with X(5) quantum number  $s = 2$ , represents the  $\beta$  bandhead

in the soft square-well potential used by that model. The applicability of this approach for the description of  $K^\pi = 0^+$  excited bands has been shown in several nuclei considered to be near the phase shape transitional point, e.g.,  $^{152}\text{Sm}$  [7],  $^{150}\text{Nd}$  [9],  $^{154}\text{Gd}$  [10],  $^{156}\text{Dy}$  [11], and  $^{178}\text{Os}$  [12].

The confined  $\beta$ -soft (CBS) rotor model, a generalization of the X(5) solution, extends the applicability of this approach to sequences of nuclides with varying stiffnesses of the potential. The CBS model describes nuclei between the X(5) shape phase transitional point and the deformed axial rotor. Like X(5), it uses a square-well potential in the deformation parameter  $\beta$ , however, now with varying boundaries in the range  $0 \leq \beta_m \leq \beta \leq \beta_M$ . The ratio  $r_\beta = \beta_m/\beta_M$  serves as its structural parameter [13]. In terms of  $r_\beta$ , the X(5) solution corresponds to  $r_\beta = 0$ , while  $r_\beta \rightarrow 1$  describes the rigid rotor limit. The CBS model was applied for the first time to the nuclei  $^{152,154}\text{Sm}$  [13]. While  $^{152}\text{Sm}$ , with  $R_{4/2} = 3.0$ , is a nucleus very close to the shape phase transitional point, its even-even neighbor  $^{154}\text{Sm}$  has an  $R_{4/2}$  value of 3.25, i.e., a value already quite close to the rigid rotor limit. The validity of the CBS model for a description of  $K_i^\pi = 0_{1,2}^+$  bands in transitional deformed nuclei with varying rotational stiffnesses ( $2.9 \leq R_{4/2} \leq 3.33$ ) has recently been justified microscopically by a comparison to the results of a relativistic mean-field model applied to the neighboring isotones  $^{150,152}\text{Nd}$  [15].

In the case of  $^{152}\text{Sm}$ , a good agreement between CBS results and experimental data on the ground state and the  $\beta$  bands was achieved [13]. This includes the excitation energies of the states and the electromagnetic transition strengths between them. In the case of  $^{154}\text{Sm}$ , the description of the properties of the ground band is also satisfactory. For the  $^{154}\text{Sm}$  first excited  $K^\pi = 0^+$  band, however, no definitive assignment as a  $\beta$  band was possible, as the experimental information on transition strengths was insufficient at the time. The lifetime of the  $0_2^+$  bandhead at 1099 keV had been measured in a Doppler shift attenuation method (DSAM) experiment, leading to a  $0_\beta^+$  assignment [16]. However, only a lower limit for the lifetime of the  $2^+$  state of the band was deduced in the same experiment. Until the present work, no information on the  $E2$  decay rates

\*tmoeller@ikp.tu-darmstadt.de

†Present address: National Superconducting Cyclotron Laboratory, Michigan State University, East Lansing, Michigan 48824, USA.

TABLE I. Summary of the results of the present measurements.

$E_{\text{Level}}$ (keV)	$J^\pi$	$J_{\text{final}}^\pi$	$E_\gamma$ (keV)	$I_\gamma$	$\delta$	sgn	$B(E2)$ (W.u.)	Literature [18] (W.u.)
82	$2_1^+$	$0_1^+$	82	— <sup>a</sup>		+		176(1)
267	$4_1^+$	$2_1^+$	185	— <sup>a</sup>		+		245(6)
		$0_1^+$	267	Not observed		+		79(3)
544	$6_1^+$	$4_1^+$	277	$3.1(2) \times 10^3$		+		289(8)
903	$8_1^+$	$6_1^+$	359	144(8)		+		319(17)
1099	$0_\beta^+$	$2_1^+$	1017	911(15)		+	11.2(21)	12(3)
1178	$2_\beta^+$	$4_1^+$	911	627(16) <sup>b</sup>		+	1.32(15)	<2.4
		$2_1^+$	1096	870(16)	$-30(21)$	−	0.72(9)	<1.3
					$-0.48(2)^c$		0.15(2) <sup>c</sup>	
		$0_1^+$	1178	557(16)		+	0.32(4)	<0.58
1338	$4_\beta^+$	$6_1^+$	795	34(3)		+	0.66(21)	
		$4_1^+$	1071	131(9)		−	0.57(18)	
		$2_1^+$	1256	164(6)		+	0.32(11)	
1440	$2_\gamma^+$	$4_1^+$	1173	139(10)		+	0.36(5)	0.48(7)
		$2_1^+$	1358	2582(61)	$-19(10)$	+	3.2(3)	
					$-0.51(7)^c$		0.65(6) <sup>c</sup>	
		$0_1^+$	1440	2076(53)		+	1.9(2)	2.13(16)
1706	$3^+$	$4_1^+$	1440	42(4)				
1815	$2^+, 3$	$2_\gamma^+$	375	46(3)				

<sup>a</sup>The intensity could not be determined with a sufficiently high accuracy.

<sup>b</sup>The transition could not be resolved from transitions nearby; the value was calculated with the branching ratio from Ref. [18].

<sup>c</sup>Disfavored alternative owing to the Alaga-rule constraint (see text).

from the  $4^+$  state of the band was available. It is the purpose of this work to fill the gap in the experimental data and allow for a direct test of the assignment of the first excited  $0^+$  band of  $^{154}\text{Sm}$  as a  $\beta$  band if the agreement with the CBS model predictions is satisfactory. To simplify our notation we use the symbols  $0_\beta^+$ ,  $2_\beta^+$ , and  $4_\beta^+$  for the energy levels at 1099, 1178, and 1338 keV, in agreement with our final conclusion (see below).

The experiment was carried out at the Argonne National Laboratory. A pulsed (12-MHz)  $^{154}\text{Sm}$  beam with an intensity of  $\sim 1$  pA was delivered by the ATLAS accelerator. The 570-MeV beam was incident on a  $630 \mu\text{g}/\text{cm}^2$   $^{12}\text{C}$  target. The total Coulomb excitation cross section amounts to about 1.7 b, as it can be estimated from the data given in Table I and the normalization discussed below. De-excitation  $\gamma$  rays, following the Coulomb excitation of the projectiles, were detected with the Gammasphere array [17], which consisted of 99 HPGe detectors arranged in 16 angular rings. Gammasphere was used in singles mode, resulting in an average total counting rate of  $9 \times 10^3$  cps, easily manageable by the Gammasphere data acquisition system. The natural  $\gamma$ -ray background is more than one order of magnitude less. A total of  $\approx 3 \times 10^8$  events of  $\gamma$ -ray fold 1 or higher was collected in about 12 h. The contribution of the natural  $\gamma$ -ray background was eliminated in the off-line data analysis by correlating the  $\gamma$  rays with the accelerator radio-frequency (rf) signal. The final spectrum is presented in Fig. 1. It is the difference between the “beam-on” (with respect to the rf) spectrum and the “beam-off” spectrum, scaled to eliminate the 1461-keV room background

transition from  $^{40}\text{K}$ . All  $\gamma$  rays in the spectrum originate from  $^{154}\text{Sm}$  nuclei recoiling with  $v/c \approx 7.85\%$ . Most of these  $\gamma$  rays have already been identified in  $^{154}\text{Sm}$  [18]. About 2% of the collected events were of  $\gamma$ -ray fold higher than 1. These data were sorted in a  $\gamma\gamma$ -coincidence matrix which was used to verify the level scheme of  $^{154}\text{Sm}$ . Levels belonging to the  $\gamma$  and  $\beta$  bands as well as negative-parity levels have been observed. The  $\gamma$ -ray lines at 637, 745, 839, 930, 1317, 1398, and 1502 keV belong to the decays of the  $5_1^-, 3_1^-, 1_1^-, 3_2^-,$  and

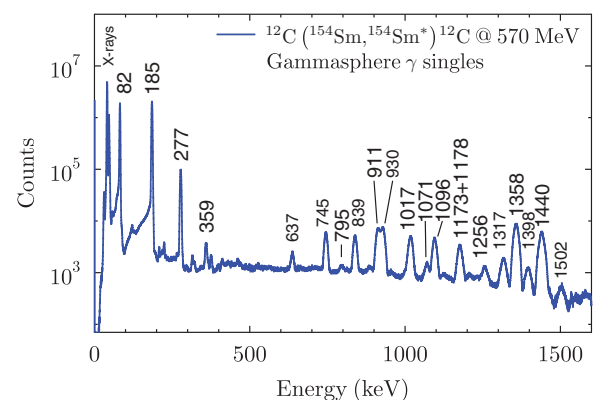


FIG. 1. (Color online) Background-subtracted, Doppler-corrected  $\gamma$ -ray singles spectrum of  $^{154}\text{Sm}$  after Coulomb excitation on a carbon target observed with the Gammasphere spectrometer. The energies of the strongest transitions are indicated.

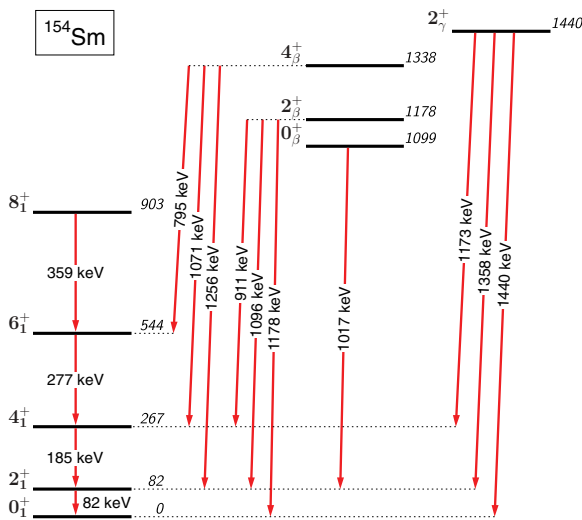


FIG. 2. (Color online) Partial level scheme of  $^{154}\text{Sm}$ .

$4_4^+$  states, respectively. In the following, we focus on the states from the  $\gamma$  and  $\beta$  bands. The spectroscopic information for these levels is summarized in Table I. A level scheme is shown in Fig. 2.

For the  $2_2^+$  state at 1178 keV and the  $2_1^+$  level at 1440 keV, an angular distribution analysis [19] was performed. The procedure is illustrated in Fig. 3 for the case of the  $2_2^+$  state, which we later use for normalization of the Coulomb

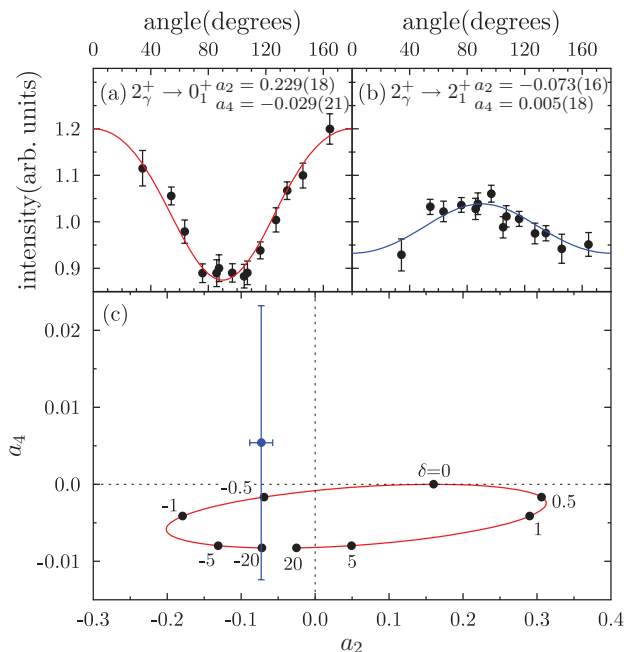


FIG. 3. (Color online) Angular distribution functions for the  $2_2^+ \rightarrow 0_1^+$  and  $2_2^+ \rightarrow 2_1^+$  transitions. Owing to background contamination, only 14 of the 16 rings were used. Solid lines are fits to a sum of Legendre polynomials. The resulting  $A_2/A_0$  and  $A_4/A_0$  coefficients for the transition  $2_2^+ \rightarrow 2_1^+$  are compared to the angular distribution ellipse, calculated with the orientation resulting from the  $A_2/A_0$  and  $A_4/A_0$  coefficients for the  $2_2^+ \rightarrow 0_1^+$  transition. The small numbers on the ellipse denote values for the  $E2/M1$  multipole mixing ratio  $\delta$ .

excitation cross sections. The intensities of the  $\gamma$  rays decaying the  $2_2^+$  and  $2_1^+$  levels were measured over the 16 rings of Gammasphere, corrected for the Lorentz boost [20] and fitted with the angular distribution function  $W(\vartheta) = A_0 + A_2 P_2(\cos \vartheta) + A_4 P_4(\cos \vartheta)$ , with  $P_n$  being the Legendre polynomials of order  $n$  [19]. The experimental  $A_2/A_0 = a_2$  and  $A_4/A_0 = a_4$  coefficients for the stretched transitions [see Fig. 3(a)] were used to unambiguously determine the statistical tensors describing the orientation of the angular momentum vectors of the states. From these, theoretical values of the coefficients  $a_2$  and  $a_4$  of the transitions to the  $2_1^+$  state were calculated for different values of the multipole mixing ratio  $\delta$ , resulting in the angular distribution ellipse depicted in Fig. 3(c). The multipole mixing ratios  $\delta$  of the transitions to the  $2_1^+$  state can then be deduced by comparing their experimentally deduced expansion coefficients [Fig. 3(b)] to the ellipse. The coefficient  $a_2$  restricts the possible  $E2/M1$  multipole mixing in the  $2_2^+ \rightarrow 2_1^+$  transition. The large uncertainty for the  $a_4$  coefficient leaves two intersections with the angular distribution ellipse within the  $1\text{-}\sigma$  interval [cf. 3(c)]. This leads to two possible values of the  $E2/M1$  multipole mixing ratio:  $\delta = -0.51(7)$ , corresponding to a 21(5)%  $E2$  contribution; and  $\delta = -19(10)$ , corresponding to an essentially pure ( $>99\%$ )  $E2$  transition. The Alaga rule, of which we assume validity to a good approximation in  $^{154}\text{Sm}$ , demands the branching ratio  $B(E2, 2_2^+ \rightarrow 2_1^+)/B(E2, 2_2^+ \rightarrow 0_1^+) \approx 1.43$ , for both possible  $K$  quantum numbers,  $K = 0$  and  $K = 2$ . From our  $\gamma$ -ray intensities, this ratio is either 0.34(3), when calculated with  $\delta = -0.51(7)$ , or 1.66(2), for  $\delta = -19(10)$ . The latter value is closer to the Alaga rule. Thus, we adopt the value of  $\delta = -19(10)$  for the mixing ratio of the  $2_2^+ \rightarrow 2_1^+$  transition. A similar argument can be made in the case of the  $2_2^+ \rightarrow 2_1^+$  transition, for which  $\delta = -30(21)$ , i.e., a  $>99\%$   $E2$  multipolarity, was adopted.

Efficiency-corrected total  $\gamma$ -ray intensities of the observed transitions were determined and used to calculate Coulomb excitation yields, normalized to the yield of the  $2_2^+$  level at 1440 keV. The yields of the excited states relative to that of the  $2_2^+$  state are proportional to the relative Coulomb excitation cross sections. The measured transition intensities are listed in Table I. The choice of the state for normalization is imposed by the fact that the  $2_1^+$  state decays to the ground state with an energy of 82 keV. In this low-energy region, the  $\gamma$ -ray detection efficiency could not be determined with suitable accuracy. The lifetime of the  $2_2^+$  state,  $\tau = 0.61(4)$  ps [16,18], is sufficiently accurate to use this level for normalization.

Electromagnetic transition matrix elements were fit to reproduce the relative Coulomb excitation yields with a multiple Coulomb excitation code [21] based on the Winther-de Boer theory [22]. An energy loss of the beam in the target of 72 MeV was taken into account. The matrix elements involved in the calculations were constrained by the experimental branching ratios and multipole mixing ratios. The known  $B(E2)$  values for the ground band [18] were included in the calculations. The relative signs of the  $E2$  matrix elements involved were derived using the square rooted Alaga rule:

$$\text{sgn} \left( \frac{\langle J_f || E2 || J_i \rangle}{\langle J_{f'} || E2 || J_i \rangle} \right) = \text{sgn} \left( \frac{\langle J_i K_i 2 \Delta K | J_f K_f \rangle}{\langle J_i K_i 2 \Delta K | J_{f'} K_{f'} \rangle} \right),$$

where  $J_i$  and  $K_i$  denote the angular momentum and angular projection quantum numbers of the initial  $i$  and final  $f$  and  $f'$  states, respectively. Previously known quadrupole moments  $Q(2_1^+) = -1.87(4)$  eb and  $Q(4_1^+) = -2.2(8)$  eb were included in the calculations [18]. For the other states, the quadrupole moment of the first  $2^+$  state was used in the analysis as a first-order approximation. The unknown intraband matrix elements for the unobserved weak transitions  $2_{\beta}^+ \rightarrow 0_{\beta}^+$  and  $4_{\beta}^+ \rightarrow 2_{\beta}^+$  have little impact on the results. This was checked by performing various Coulomb excitation calculations. Nevertheless, the theoretical expectations from Ref. [13] were assumed for these unobserved transitions in the further analysis. The absolute scale for the resulting transition strengths is given by the lifetime of  $0.61(4)$  ps of the  $2_{\gamma}^+$  state [16,18], which, together with the new  $\gamma$ -ray branching ratios from our data, results in a transition strength of  $B(E2; 2_{\gamma}^+ \rightarrow 0_1^+) = 1.9(2)$  W.u. and a Coulomb excitation cross section  $\sigma(2_{\gamma}^+) = 2.8(3)$  mb.

The calculations resulted in the determination of 10 absolute  $E2$  transition strengths, summarized in Table I. The new values are in good agreement with the previously measured values or limits. For the  $0_{\beta}^+$  state, the newly determined value for the lifetime of  $1.37(26)$  ps compares well with that from DSAM experiments [ $1.3(3)$  ps] [16]. This agreement further supports our choices for the yield normalization and for the signs of the matrix elements.

The results contain the first data on lifetimes of states in the low-energy part of the  $\beta$  band, which are summarized and compared with the predictions of the X(5) description and the CBS rotor model using  $r_{\beta} = 0.35$  [13] in Table II. As expected, the X(5) scheme cannot accurately reproduce the experimental  $B(E2)$  values in the  $\beta$  band of  $^{154}\text{Sm}$  because this nucleus exhibits a more rotor-like behavior than assumed by that model. The agreement with the CBS model predictions [13] is better, except for the ( $\Delta J = +2$ ) transitions,  $2_{\beta}^+ \rightarrow 4_1^+$  and  $4_{\beta}^+ \rightarrow 6_1^+$ ; these are overestimated by the CBS model by a factor of 5–12. On the other hand, the  $4_{\beta}^+ \rightarrow 2_1^+$ ,  $4_{\beta}^+ \rightarrow 4_1^+$ ,  $2_{\beta}^+ \rightarrow 2_1^+$ ,  $2_{\beta}^+ \rightarrow 0_1^+$ , and  $0_{\beta}^+ \rightarrow 2_1^+$   $E2$  transition rates are predicted well by the CBS rotor model. The general agreement between the CBS model predictions in Ref. [13] and the data, on both the transitional nucleus  $^{152}\text{Sm}$  [7,13] and the rotational nucleus  $^{154}\text{Sm}$  studied here, demonstrates the ability of the CBS rotor model to describe in a satisfactory way the properties of  $K=0$  bands in nuclei on the path from the X(5) shape phase transitional point to the rigid rotors. The key characteristic of the model description of the states belonging to this band is that they represent excitations in the deformation parameter  $\beta$ . Owing to the satisfactory agreement between the predictions

TABLE II. Comparison of the experimentally deduced  $E2$  transition strengths for states in the  $\beta$  band with the theoretical predictions available in the literature from the X(5) description [5] and from the CBS rotor model ( $r_{\beta} = 0.35$ ) [13].

$J_i \rightarrow J_f$	$E_x(J_i)$ (keV)		$B(E2)$ (W.u.)		
	CBS	Expt.	X(5) [5] <sup>a</sup>	CBS [13]	Expt.
$2_1^+ \rightarrow 0_1^+$	82	82	176	174	176(1) <sup>b</sup>
$4_1^+ \rightarrow 2_1^+$	268	267	278	251	245(6) <sup>b</sup>
$6_1^+ \rightarrow 4_1^+$	546	544	348	281	289(8) <sup>b</sup>
$8_1^+ \rightarrow 6_1^+$	903	903	400	300	319(17) <sup>b</sup>
$0_{\beta}^+ \rightarrow 2_1^+$	1231	1099	111	8.4	11.2(21)
$2_{\beta}^+ \rightarrow 0_1^+$	1325	1178	3.5	0.5	0.32(4)
$2_{\beta}^+ \rightarrow 2_1^+$			16	1.4	0.72(9)
$2_{\beta}^+ \rightarrow 4_1^+$			63	7.1	1.32(15)
$4_{\beta}^+ \rightarrow 2_1^+$	1546	1338	1.8	0.1	0.32(11)
$4_{\beta}^+ \rightarrow 4_1^+$			11	1.1	0.57(18)
$4_{\beta}^+ \rightarrow 6_1^+$			49	8.2	0.66(21)

<sup>a</sup>Scaled to the  $B(E2; 2_1^+ \rightarrow 0_1^+)$  value.

<sup>b</sup>Value from Ref. [18].

by the CBS model obtained previously [13] and our new data, we conclude that the  $0_2^+$  state of the strongly deformed nucleus  $^{154}\text{Sm}$  is one of the rare cases correctly assigned [16] as the  $0_{\beta}^+$  vibrational state. In order to further support our assignment it would be desirable to identify a two-phonon  $\beta$ -vibrational band of  $^{154}\text{Sm}$  that would decay more strongly to the one-phonon  $\beta$  band than to the ground state.

In summary, we have studied  $^{154}\text{Sm}$  using projectile-Coulomb excitation. The data yield 10 absolute  $E2$  transition strengths including the complete set of seven  $B(E2)$  values to the ground-state band for the first three members of the  $\beta$  band. The experimental results for the excited  $K^{\pi} = 0^+$  band are in good agreement with the predictions of the CBS model for the  $\beta$  band of this nucleus and thus establish the assignment of the first  $K^{\pi} = 0^+$  band of  $^{154}\text{Sm}$  as a  $\beta$  band.

This work was supported by the DFG under Grant Nos. Pi 393/2-2 and SFB 634, by the German-Bulgarian exchange program under Grant Nos. PPP 50751591 and DNTS/01/2/2011, by the BgNSF under Grant No. DO 02-219, by the Alexander von Humboldt Foundation, and by the Helmholtz International Center for FAIR. The work at Argonne National Laboratory was supported by the US Department of Energy, Office of Nuclear Physics, under Contract No. DE-AC02-06CH11357.

- [1] A. Bohr, *Mat. Fys. Medd. K. Dan. Vidensk. Selsk.* **26**, 14 (1952).  
 [2] L. Wilets and M. Jean, *Phys. Rev.* **102**, 788 (1956).  
 [3] F. Iachello, *Phys. Rev. Lett.* **85**, 3580 (2000).  
 [4] D. Bonatsos, D. Lenis, N. Pietralla, and P. A. Terziev, *Phys. Rev. C* **74**, 044306 (2006).  
 [5] F. Iachello, *Phys. Rev. Lett.* **87**, 052502 (2001).  
 [6] F. Iachello, *Phys. Rev. Lett.* **91**, 132502 (2003).

- [7] R. F. Casten and N. V. Zamfir, *Phys. Rev. Lett.* **87**, 052503 (2001).  
 [8] A. Bohr and B. Mottelson, *Nuclear Deformations, Nuclear Structure* (World Scientific, Singapore, 1998).  
 [9] R. Krücken, B. Albanna, C. Bialik, R. F. Casten, J. R. Cooper, A. Dewald, N. V. Zamfir, C. J. Barton, C. W. Beausang, M. A. Caprio *et al.*, *Phys. Rev. Lett.* **88**, 232501 (2002).

- [10] A. Dewald, O. Möller, D. Tonev, A. Fitzler, B. Saha, K. Jessen, S. Heinze, A. Linnemann, J. Jolie, K. Zell *et al.*, *Eur. Phys. J. A* **20**, 173 (2003).
- [11] O. Möller, A. Dewald, P. Petkov, B. Saha, A. Fitzler, K. Jessen, D. Tonev, T. Klug, S. Heinze, J. Jolie *et al.*, *Phys. Rev. C* **74**, 024313 (2006).
- [12] A. Dewald, O. Möller, B. Saha, K. Jessen, A. Fitzler, B. Melon, T. Pissulla, S. Heinze, J. Jolie, K. O. Zell *et al.*, *J. Phys. G: Nucl. Part. Phys.* **31**, S1427 (2005).
- [13] N. Pietralla and O. M. Gorbachenko, *Phys. Rev. C* **70**, 011304 (2004).
- [14] K. Dusling and N. Pietralla, *Phys. Rev. C* **72**, 011303 (2005).
- [15] A. Krugmann, Z. P. Li, J. Meng, N. Pietralla, and D. Vretenar, *J. Phys. G: Nucl. Part. Phys.* **38**, 065102 (2011).
- [16] R. Krücken, C. J. Barton, C. W. Beausang, R. F. Casten, G. Cata-Danil, J. R. Cooper, J. Novak, L. Yang, M. Wilhelm, N. V. Zamfir *et al.*, *Phys. Lett. B* **454**, 15 (1999).
- [17] I. Y. Lee, *Nucl. Phys. A* **520**, c641 (1990).
- [18] C. W. Reich, *Nucl. Data Sheets* **110**, 2257 (2009).
- [19] T. Yamazaki, *Nucl. Data Sec. A* **3**, 1 (1967).
- [20] A. E. Stuchbery, *Nucl. Phys. A* **723**, 69 (2003).
- [21] H. Ower, Ph.D. thesis, Johann Wolfgang zu Goethe Universität zu Frankfurt am Main, 1980.
- [22] A. Winther and J. de Boer, *A Computer Program for Multiple Coulomb Excitation* (Academic Press, New York, 1966), p. 303.